ETHZ-ITP PR/94-1

THE LOW-ENERGY PION-NUCLEON INTERACTION

P.F.A. Goudsmit, H.J. Leisi and E. Matsinos

Institute for Particle Physics (ITP), ETH Zürich,
CH-5232 Villigen PSI, Switzerland

(submitted for publication in Nuclear Physics A)

Institute for Particle Physics
ETH Zürich
5232 Villigen PSI
Switzerland

The low-energy pion-nucleon interaction

P.F.A. Goudsmit, H.J. Leisi and E. Matsinos

Institute for Particle Physics, ETH Zurich, CH-5232 Villigen PSI, Switzerland

Abstract

With our pion-nucleon interaction model, based on σ, ρ, N and Δ-isobar exchanges, we calculate differential, 'partial-total' or total cross sections and the analyzing powers for all the low-energy elastic-scattering and single-charge-exchange data recently published. We conclude that the model provides a very good description of the (low-energy) pion-nucleon interaction. The comparison of the model predictions and the experimental results reveals that there are contradictions between the old data base and some of the recently published data.

Submitted to Nuclear Physics A.

1 Introduction

During the last ten years, Pion Physics has rather become a problematic field. The pion-nucleon ($\pi - N$) differential-cross-section measurements below pion lab kinetic energies of about 100 MeV, accumulated at the three meson factories (LAMPF, PSI, TRIUMF) during this period, are (in some occasions) in severe disagreement [1] with the data base of the late seventies; furthermore, contradictions among the recently obtained data sets are also present.

In refs. [2]-[4], we developed a $\pi - N$ interaction model. This is the first relativistic point-hadron $\pi - N$ model which accounts for all the processes $\pi N \rightarrow \pi' N'$ (elastic scattering and single-charge exchange) from threshold up to the energy of the Δ_{33} resonance. The model, which also accounts for the $\pi - N$ Σ-term, is based on σ (scalar-isoscalar) and ρ (vector-isovector) t-channel exchanges and on s- and u-channel graphs with a nucleon and a Δ-isobar in the intermediate state.

The seven parameters of the model are: G_σ, $G_\rho^{(V)}$, κ, $g_{\pi NN}$, x, $g_{\pi N\Delta}$ and Z. G_σ describes the σ exchange, $G_\rho^{(V)}$ pertains to the vector part of the ρ exchange and κ denotes the ratio between the tensor and the vector $\rho - N$ coupling constants. The remaining four parameters are associated with the s- and u-channel exchanges; $g_{\pi NN}$ is the $\pi - N$ coupling constant, x stands for the pseudoscalar admixture in the πNN vertex, $g_{\pi N\Delta}$ denotes the $\pi N\Delta$ coupling constant and the parameter Z determines the spin-$\frac{1}{2}$ admixture in the Δ-isobar field.

The parameters of the model have been mainly [1] determined after fitting to the

[1] The measured $1s$ level shift of pionic hydrogen [5] has been used as a constraint in our fit; assuming that isospin symmetry holds in the strong interactions, this measurement leads to $b_0(0) - b_1(0) =$

phase-shift results by Koch and Pietarinen [6] (the KH80 solution) for pion CM kinetic energies between 15 and 75 MeV. The input errors have been determined through the comparison of the KH80 solution with the results by Bugg [7].

It has been proven that this model not only describes perfectly all s- and p-wave phase shifts in the fitting region, but also correctly predicts their energy dependence up to the Δ_{33} resonance. Moreover, the predictions of the model for the p-wave scattering volumes are in perfect agreement (at the 1% level) with those of ref. [8] (the KA85 solution), while the two corresponding predictions for the isovector s-wave scattering length $b_1(0)$ differ [2] by about 10%.

Once the parameters of the model are fixed, one can then calculate any observable (differential, 'partial-total' or total cross section and analysing power) for the $\pi - N$ elastic-scattering and single-charge-exchange reactions with the help of the formulae of ref. [4]. The purpose of the present work is twofold. First, we attempt to test our model further by comparing its predictions with the 'new' experimental results; the information content of these data is not contained in the model parameters since the latter have been determined from the phase-shift solution KH80. Second, we aim at making a contribution to the long-standing problem in the low-energy Pion Physics, namely the apparently conflicting results among different experimental groups [1]. One difficulty, associated with the problem, is that the different experiments are not (in general) performed at the same values of the kinematic quantities (angles and

$0.086 \pm 0.004\ m_\pi^{-1}$, where $b_0(0)$ and $b_1(0)$ denote the standard isoscalar and isovector scattering lengths.

[2]Current and future experiments at PSI on pionic hydrogen and deuterium [9] should provide a direct determination of both the scattering lengths $b_0(0)$ and $b_1(0)$.

energies) and, therefore, their results are not directly comparable. Since the cross sections are calculated with our model for the conditions of each particular experiment precisely, it is possible for us to interrelate the various experimental data by means of our predictions. Also, an interrelation (through the model predictions) of the different reactions becomes possible. Strictly speaking, we are able to interrelate the 'old' data base (i.e. those experiments which served as input to the KH80 phase-shift solution) and the various 'new' experimental data.

This analysis is confined to the low-energy region, i.e. to pion lab kinetic energies T_π between 20 and 100 MeV (corresponding to pion CM kinetic energies ε of about 15 and 70 MeV, respectively) for three reasons:

- the natural region of applicability of our model (where one expects high predictive power) is the low-energy one; this is due to its construction,
- it is exactly in this region that discrepancies among the experimental results persist and
- the low-energy region is the most interesting place to study the symmetry properties of QCD (chiral symmetry, isospin symmetry).

The low-energy limit ($T_\pi^{min} = 20\ MeV$) is dictated by the availability of the experimental data and the difficulty of performing the electromagnetic corrections at lower energies.

2 The sensitivity of the parameters of the model on the phase-shift solutions

Before embarking on the program of comparing the 'new' $\pi - N$ measurements with the predictions of our model, we will investigate the sensitivity of our parameters to the particular set of phase shifts used as input in our fit. As mentioned above, up to now (refs. [3] and [4]), the fit was performed to the KH80 phase shifts [6] for pion CM kinetic energies between 15 and 75 MeV. Now, we will also fit to the KA85 phase-shift results [8] in the same energy domain. The comparison between the two corresponding sets of parameter values will provide an idea about the sensitivity of our results to the input data.

The standard MINUIT routines have been used once more. As expected, there is insensitivity to the parameter $G_\rho^{(V)}$; as also done in refs. [3] and [4], this parameter has been varied between 30 and 60 GeV^{-2} (with a step of 5 GeV^{-2}) and, for each particular $G_\rho^{(V)}$-value, a six-parameter fit was performed. No significant changes either in the parameter values or in the quality of the fit have been observed when shifting from the KH80 to the KA85 solution.

Table 1 shows one typical example of the differences for these two choices of the phase-shift solution (with $G_\rho^{(V)}$ fixed at Pietarinen's value [3]). From this table, we conclude that,

- the χ^2/NDF-value of the fit is smaller for the KA85 data, this being a result of

[3]For the $\rho - N$ vector coupling constant $g_{\rho NN}^{(V)}$ fixed at Pietarinen's value [10] and for the $\pi - \rho$ coupling constant $g_{\pi\pi\rho}$ determined from the ρ-meson decay width, a value of 54.1 GeV^{-2} for $G_\rho^{(V)}$ can be obtained; hereafter, we will refer to this value as Pietarinen's value for $G_\rho^{(V)}$.

the 'smoothening' process 'imposed' on the KA85 solution by the stronger (in this case) theoretical constraints, and

• the values of the parameters do not change beyond the quoted uncertainties, with the marginal exception of the parameter $g_{\pi NN}$ (which changes by slightly more than one standard deviation).

With $G_{\rho}^{(V)}$ fixed (again) at Pietarinen's value, we show the energy dependence of the s- and p-wave phase shifts (figs. 1) and of the real parts of the coefficients of the $\pi - N$ scattering amplitude (figs. 2) in the fitting region. The largest differences between the two solutions correspond to the case of the small phase shift $\delta(P_{11})$ and amount up to 20% at $\varepsilon \sim 80\ MeV$.

From the above, we can conclude that the predictions of our model are insensitive to the choice of the particular phase-shift analysis. In the following, we will make use of the parameter values as determined from the fit to the KH80 phase shifts.

3 Our model and the 'new' experimental data

In this Section, we compare the predictions of our model with the 'new' measurements of the differential, 'partial-total' (often also referred to as 'integral') or total cross sections and of the analyzing powers for the two elastic $\pi^{\pm}p$ and for the single-charge-exchange ($\pi^- p \rightarrow \pi^0 n$) reactions. All data, shown here, are the results of experiments conducted after 1980; only refereed articles have been taken into account.

The differential cross sections and the analyzing powers are functions of two kinematic variables; in the following, these variables are chosen to be the CM scattering angle θ and the pion lab kinetic energy T_{π}. The 'partial-total' or total cross sections are, of course, functions of T_π, exclusively. In all cases, four partial waves were considered (s, p, d and f). The values of all the physical constants have been taken from ref. [11]. The electromagnetic effects have been treated according to the NORDITA algorithm [12].

In all the figures in the present analysis, the solid curves represent the prediction of our model; they correspond to the average value of the particular observable in question (differential cross section, 'partial total' or total cross section and analyzing power) when $G_\rho^{(V)}$ varies between 30 and 60 GeV^{-2}. The dotted curves in the figures designate the extent of the 'systematic' uncertainties (they actually reflect the uncertainty of the input phase-shift data); they have been calculated in the same way as in refs. [3] and [4]: for a specific value of $G_\rho^{(V)}$ (varying between 30 and 60 GeV^{-2} with a step of 5 GeV^{-2}), values for the remaining six parameters of our model were produced randomly in normal distributions after taking into account the results of our fits (mean values, errors, as well as the correlation between G_σ and Z [4]). The errors, quoted for each observable, correspond to the r.m.s. deviation in the corresponding distributions.

The experimental errors, shown in the figures, are purely statistical, except mentioned otherwise; they do not include the normalization uncertainties. Some interesting information, concerning these experiments, may be found in tables 2 and 3.

[4]The correlation coefficients between any other pair of these six parameters are significantly smaller and were ignored.

3.1 The elastic π^+p reaction

3.1.1 Differential cross sections

The RITCHIE83 data [13] (fig. 3(a)) The agreement between the experimental data and the prediction of the model is excellent. Only the 72.5 MeV measurements are slightly lower (than the corresponding predictions), yet the effect is not statistically significant. The signal-to-noise ratio for these measurements is low (ranging between $\frac{1}{2}$ and 2).

The FRANK83 data [14] (fig. 3(b)) One needs large correction factors (in comparison to the normalization uncertainties quoted) for two of the data sets (namely, the measurements at 29.4 and 89.6 MeV) in order to achieve agreement with the model. Due to their large normalization uncertainties, the data at 49.5 and at 69.6 MeV are not very useful.

The BRACK86 data [15] (figs. 3(c)) The authors claim very small normalization uncertainties for all four data sets. The experimental errors, shown in the figures, represent counting statistics as well as the uncertainty in the effective detector solid angle determined by a Monte-Carlo process. A small uncertainty of ± 0.5 MeV in the incident pion kinetic energy has not been included. It is evident that the disagreement between the data and the prediction of the model is serious at all energies.

The BRACK88 data [16] (fig. 3(d)) The measurements are consistent with the previous experiment [15] by the group and sustain the sheer disagreement between the data and the prediction of the model.

The WIEDNER89 data [17] (fig. 3(e)) This single-energy experiment was performed in the Coulomb interference region (forward scattering). The authors report a normalization uncertainty of 6.5 %. The agreement between the data and the prediction of the model is excellent. The experimental errors, shown in this figure, include the statistical uncertainties as well as systematic errors resulting from background subtraction and uncertainties in the knowledge of the scattering angle.

The BRACK90 data [18] (fig. 3(f)) The measurements at 66.8 MeV are consistent with the previous results by the group ([15] and [16]). Furthermore, they extend to smaller angles and result to a **different shape** of the angular distribution (to the one predicted by the model); apparently, the agreement with the model is not a question of renormalization of the experimental data anymore. The data at 45 MeV also disagree with the model (however, not in shape), whereas the data at 30 MeV are rather consistent with the model prediction. The errors, shown in the figures, represent counting statistics and statistical uncertainties in the effective counter solid angle and effective target thickness determined by a Monte-Carlo process. Again, a small uncertainty of ± 0.5 MeV in the incident pion kinetic energy has not been included.

3.1.2 'Partial-total' cross sections

The experimental results of ref. [19] for the elastic $\pi^+ p$ 'partial-total' cross section are shown, along with the prediction of our model, in figs. 4. The two low-energy entries (at 45 and 51.5 MeV) of ref. [19] are not considered to be reliable [20] and have not been included in fig. 4(b). The agreement is very good.

3.1.3 Analyzing power

The SEVIOR89 data [21] (fig. 5) There is an excellent agreement between the experimental data and the predictions of the model. Statistical and systematic errors are combined.

3.2 The elastic $\pi^- p$ reaction

3.2.1 Differential cross sections

The FRANK83 data [14] (figs. 6(a)). In general, the measurements agree with the prediction of the model. The experimental data at 29.4 MeV are slightly, yet systematically, lower than our prediction. The measurements at 89.6 MeV are significantly lower; however, the normalization uncertainty (corresponding to this data set) is large.

The BRACK86 data [15] (figs. 6(b)) The deviations (from the model predictions) can rather be accounted for by the uncertainties (i.e. the ones associated with our prediction and the experimental ones) in all four pion energies. The errors, shown in the figures, are identical to the ones in the corresponding $\pi^+ p$ case.

The WIEDNER89 data [17] (fig. 6(c)) The deviations between the model and the experimental measurements are (on average) a factor of two larger than the normalization uncertainty claimed by the authors. The trend of the data is systematic. The errors, shown in the figure, are identical to the ones in the corresponding $\pi^+ p$ case.

The BRACK90 data [18] (figs. 6(d)) The differences can be accounted for by the uncertainties, both the experimental ones and the ones related to our prediction in all cases. The errors, shown in the figures, are identical to the ones in the corresponding

π^+p case.

3.2.2 Analyzing power

The ALDER83 data [22] (fig. 7) In view of the large experimental uncertainties (which, however, do not include the errors on the target polarization), the agreement between the experimental data and the predictions of the model is good.

The SEVIOR89 data [21] (fig. 7) The agreement between the experimental data and the predictions of the model is excellent. Statistical and systematic errors are combined.

3.3 The single-charge-exchange reaction

3.3.1 Differential cross sections

The FITZGERALD86 data [23] (figs. 8) The discrepancies (between the experimental data and the prediction of the model) decrease with increasing energy. The trend is systematic; in all cases, the measurements exceed the predictions. The errors, shown in the figures, represent the counting statistics and detector solid-angle uncertainties.

3.3.2 Total cross section

In fig. 9, the experimental results of refs. [24] and [25] are shown along with the prediction of our model. The trend of the data is systematic (i.e. the measurements are lower than the corresponding predictions by about one standard deviation).

4 Discussion

As far as the π^+p differential cross sections are concerned, there is a sheer disagreement of the experimental data of FRANK83 (at 29.4 and at 89.6 MeV) and of all the TRIUMF measurements (with the possible exception of the 30 MeV data in the BRACK90 measurements) with the prediction of our model. The trend of the data is systematic: the measured differential cross sections are lower than the corresponding predictions [5]. In all but one cases of disagreement (i.e. exempting the 66.8 MeV data in the BRACK90 measurements), the agreement between the model and the experimental results can be achieved by means of the strong renormalization of the data (i.e. by the application of a correction factor much larger than the corresponding normalization uncertainties). For the BRACK90 66.8 MeV measurements, this is not the case; the shape of the measured differential cross section is different to the predicted one.

As far as the π^-p differential cross sections are concerned, the existing discrepancies can be rather accounted for by the uncertainties (i.e. the ones associated with our prediction and the experimental ones). In this respect, only the WIEDNER89 data seem to be somewhat problematic; for this data set, the differences between our prediction and the measurements disappear in case that the experimental results are renormalized by applying a correction factor twice as big as the normalization uncertainty claimed by the authors.

Unfortunately, the differential cross-section values for the single-charge-exchange

[5] It is worth noting that recent π^+p differential-cross-section measurements [26], conducted at PSI, also seem to support lower values (than the ones predicted by the model).

reaction in the low-energy region have been presented in a tabulated form by only one experimental group (the FITZGERALD86 data). For these measurements, the trend of the data is systematic; the experimental results exceed the model predictions. The deviations decrease with increasing energy.

The experimental results of the π^+p 'partial-total' cross sections in the low-energy region (ref. [19]) yields consistent results with our model [6]. The TRIUMF π^+p differential-cross-section measurements (refs. [15], [16] and [18]) and the 'partial-total' cross-section ones (also measured at TRIUMF) contradict one another. At least one of the two sets of measurements has to be erroneous.

The measurements of the total cross sections, corresponding to the single-charge-exchange reaction, are slightly, yet systematically, lower than the model predictions (the differences being of the order of one standard deviation).

As far as polarization measurements are concerned, the agreement between the prediction of our model and the existing experimental data is excellent. Since polarization measurements are sensitive to the interference between amplitudes, thus being sensitive to the small (non-resonant) partial waves, this agreement is interpreted as an (additional) evidence that the small phase shifts are properly accounted for with our model.

To review: the experimental status of the low-energy $\pi - N$ interaction is far from settled, despite the abundance of the data at the meson factories and the supposed

[6]However, recent preliminary data of an experiment at LAMPF [27] on π^+p 'partial-total' cross sections disagree with the conclusions of ref. [19]. The corresponding (preliminary) π^-p measurements (the first ones to be conducted in the low-energy region) are also reported to be inconsistent with the KH80 phase-shift solution.

improvement of both the experimental techniques and the efficiency and reliability of the detectors during the last two decades. From this point of view, the still persisting discrepancies are rather astonishing.

5 Conclusions and prospects

The comparison between the model predictions (no free parameter!) and the 41 experimental curves (figs. 3 - 9) shows that the bulk of the experimental data and the model predictions agree within the respective errors. In most cases of disagreement, the shape of the predicted curve follows the trend of the experimental results; in these cases, a renormalization of the data (usually beyond the normalization uncertainties claimed by the various experimental groups) restores agreement. There is only one case where there is disagreement in shape. From all the above, we conclude that our dynamical model provides a **very good description of the low-energy $\pi - N$ interaction.**

We do not imply that in the cases of disagreement the recent experimental data are necessarily erroneous; the discrepancies simply indicate that the old data base (used as input to the KH80 and KA85 solutions) is not consistent with some of the recent experimental results. The erroneous data could be either some of the new data or the data pertaining to the old data base (together with the recent experimental data sets which agree with it!). The situation, concerning $\pi^- p$ elastic scattering, is rather satisfactory: within the respective errors, there seems to be hardly any disagreement between the model prediction and the experimental data.

If isospin symmetry holds in the strong interactions, then the two elastic-scattering

($\pi^{\pm}p$) and the single-charge-exchange reactions are described by only two scattering amplitudes (namely, the isospin-$\frac{3}{2}$ and the isospin-$\frac{1}{2}$ ones) for each spin-parity channel. Isospin symmetry is implemented in the present form of our model. Provided that the electromagnetic corrections are properly described by the NORDITA algorithm and that the experimental results are reliable, then the observed deviations (between the model prediction and the experimental data for different reactions) could be attributed to isospin-symmetry breaking in the strong interactions.

There are two regions in which the error band of the model prediction appears to be larger than the precision of the experimental measurements: the $\pi^{-}p$ elastic scattering at backward angles (figs. 6(b) and 6(d)) and the single-charge-exchange reaction at forward angles (figs. 8). These two regions are under current study.

One of us (E.M.) acknowledges helpful discussions with M.E. Sainio.

References

[1] G. Höhler, πN Newsletter **2** (1990) 1; G. Höhler and J. Stahov, πN Newsletter **2** (1990) 42; D.V. Bugg, πN Newsletter **3** (1991) 1, ed. R.E. Cutkosky, G. Höhler, W. Kluge and B.M.K. Nefkens

[2] P.F.A. Goudsmit, H.J. Leisi and E. Matsinos, Phys. Lett. **B271** (1991) 290

[3] P.F.A. Goudsmit, H.J. Leisi and E. Matsinos, Phys. Lett. **B299** (1993) 6

[4] P.F.A. Goudsmit, H.J. Leisi, E. Matsinos, B.L. Birbrair and A.B. Gridnev, ETHZ-IMP preprint 93-2; a revised version of the preprint has been submitted to Nuclear Physics A

[5] W. Beer et al., Phys. Lett. **B261** (1991) 16

[6] R. Koch and E. Pietarinen, Nucl. Phys. **A336** (1980) 331

[7] D.V. Bugg, πN Newsletter **6** (1992) 7, ed. R.E. Cutkosky, G. Höhler, W. Kluge and B.M.K. Nefkens

[8] R. Koch, Nucl. Phys. **A448** (1986) 707

[9] A. Badertscher et al., Nucl. Instr. **A335** (1993) 470; πN Newsletter **8** (1993) 168, ed. G. Höhler, W. Kluge and B.M.K. Nefkens

[10] O. Dumbrajs et al., Nucl. Phys. **B216** (1983) 277; the $g^{(V)}_{\rho NN}$ values have been corrected by a factor of two (G.C. Oades, private communication, 1991)

[11] 'Review of Particle Properties', Phys. Rev. **D45** (1992) 1

[12] B. Tromborg, S. Waldenstrøm, I. Øverbø, Phys. Rev. **D15** (1977) 725; Helv. Phys. Acta **51** (1978) 584

[13] B.G. Ritchie et al., Phys. Lett. **B125** (1983) 128

[14] J.S. Frank et al., Phys. Rev. **D28** (1983) 1569

[15] J.T. Brack et al., Phys. Rev. **C34** (1986) 1771

[16] J.T. Brack et al., Phys. Rev. **C38** (1988) 2427

[17] U. Wiedner et al., Phys. Rev. **D40** (1989) 3568

[18] J.T. Brack et al., Phys. Rev. **C41** (1990) 2202

[19] E. Friedman et al., Nucl. Phys. **A514** (1990) 601

[20] E. Friedman, private communication (November 1993)

[21] M.E. Sevior, Phys. Rev. **C40** (1989) 2780

[22] J.C. Alder, Phys. Rev. **D27** (1983) 1040

[23] D.H. Fitzgerald, Phys. Rev. **C34** (1986) 619

[24] A. Bagheri et al., Phys. Rev. **C38** (1988) 885

[25] M. Salomon et al., Nucl. Phys. **A414** (1984) 493

[26] M. Metzler et al., πN Newsletter **2** (1990) 32; C. Joram et al., πN Newsletter **2** (1990) 39; C. Joram et al., πN Newsletter **3** (1991) 22; C. Joram, πN Newsletter **5** (1992) 117, ed. R.E. Cutkosky, G. Höhler, W. Kluge and B.M.K. Nefkens; C.

Joram et al., πN Newsletter **8** (1993) 30, ed. G. Höhler, W. Kluge and B.M.K. Nefkens

[27] B.J. Kriss et al., πN Newsletter **8** (1993) 17, ed. G. Höhler, W. Kluge and B.M.K. Nefkens

Figure caption

Figures 1:

The energy dependence of the s- and p-wave phase shifts in the fitting region for $G_\rho^{(V)}$ fixed at Pietarinen's value. Along with the KH80 [6] (plus signs) and the KA85 [8] (crosses) data, the results by Bugg [7] (diamonds) are also shown. Solid lines: fit to the KH80 results, dotted lines: fit to the KA85 results.

Figures 2:

The energy dependence of the real parts of the coefficients of the $\pi - N$ scattering amplitude in the fitting region for $G_\rho^{(V)}$ fixed at Pietarinen's value. Along with the KH80 [6] (plus signs) and the KA85 [8] (crosses) data, the results by Bugg [7] (diamonds) are also shown. Solid lines: fit to the KH80 results, dotted lines: fit to the KA85 results.

Figures 3:

The elastic $\pi^+ p$ differential cross sections as functions of the scattering angle. The experimental data correspond to refs. [13]-[18]. In each figure, the pion lab kinetic energy and the normalization uncertainty are quoted (the latter in parentheses). The solid line represents the prediction of our model. The dotted lines are indicative of the uncertainty in our prediction.

Figures 4:

The predictions of our model for the π^+p 'partial-total' cross section along with the experimental data from ref. [19]. The minimum lab angle θ^{lab}_{min}, considered for the integration, is 20 degrees (fig. 4(a)) and 30 degrees (fig. 4(b)). The two low-energy entries (at 45 and 51.5 MeV) of ref. [19] are not considered as reliable [20] and have not been included in fig. 4(b). The dotted lines are indicative of the uncertainty in our prediction.

Figure 5:

The π^+p asymmetry parameter A, measured in ref. [21], along with the prediction of our model for the polarization coefficient P; if isospin symmetry holds in the strong interactions, then the two quantities are identical [21]. The solid line represents the prediction of our model. The dotted lines are indicative of the uncertainty in our prediction.

Figures 6:

The elastic π^-p differential cross sections as functions of the scattering angle. The experimental data correspond to refs. [14], [15], [17] and [18]. In each figure, the pion lab kinetic energy and the normalization uncertainty are quoted (the latter in parentheses). The solid line represents the prediction of our model. The dotted lines are indicative of the uncertainty in our prediction.

Figure 7:

The $\pi^- p$ asymmetry parameter A, measured in refs. [21] and [22], along with the prediction of our model for the polarization coefficient P; if isospin symmetry holds in the strong interactions, then the two quantities are identical [21]. The solid line represents the prediction of our model. The dotted lines are indicative of the uncertainty in our prediction.

Figures 8:

The single-charge-exchange differential cross sections as functions of the scattering angle. The experimental data correspond to ref. [23]. In each figure, the pion lab kinetic energy and the normalization uncertainty are quoted (the latter in parentheses). The solid line represents the prediction of our model. The dotted lines are indicative of the uncertainty in our prediction.

Figure 9:

The predictions of our model for the single-charge-exchange total cross section along with the experimental data from refs. [24] and [25]. The dotted lines are indicative of the uncertainty in our prediction.

Figs. 1

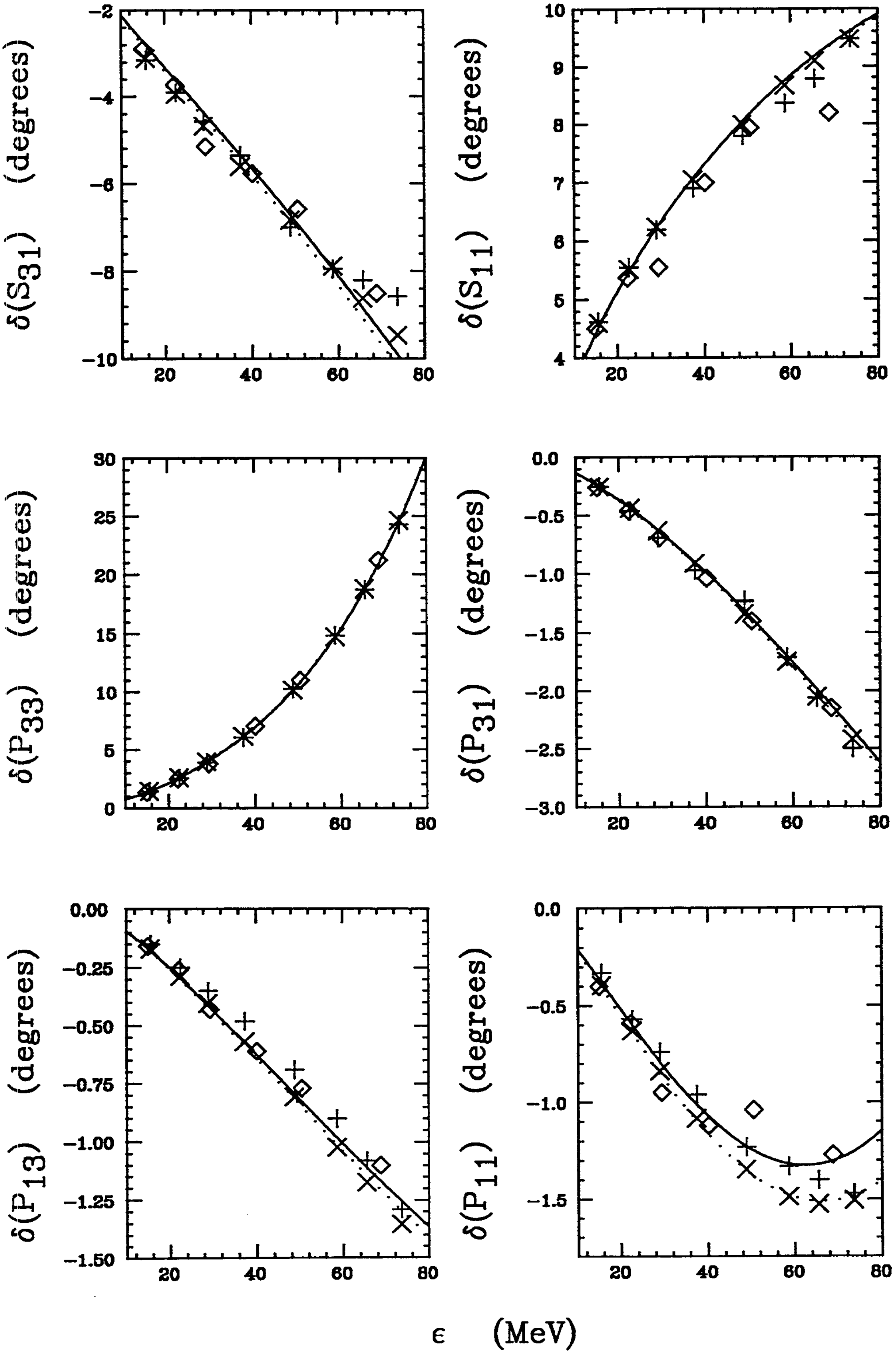

δ(S31) (degrees)
δ(S11) (degrees)
δ(P33) (degrees)
δ(P31) (degrees)
δ(P13) (degrees)
δ(P11) (degrees)
ε (MeV)

Figs. 2

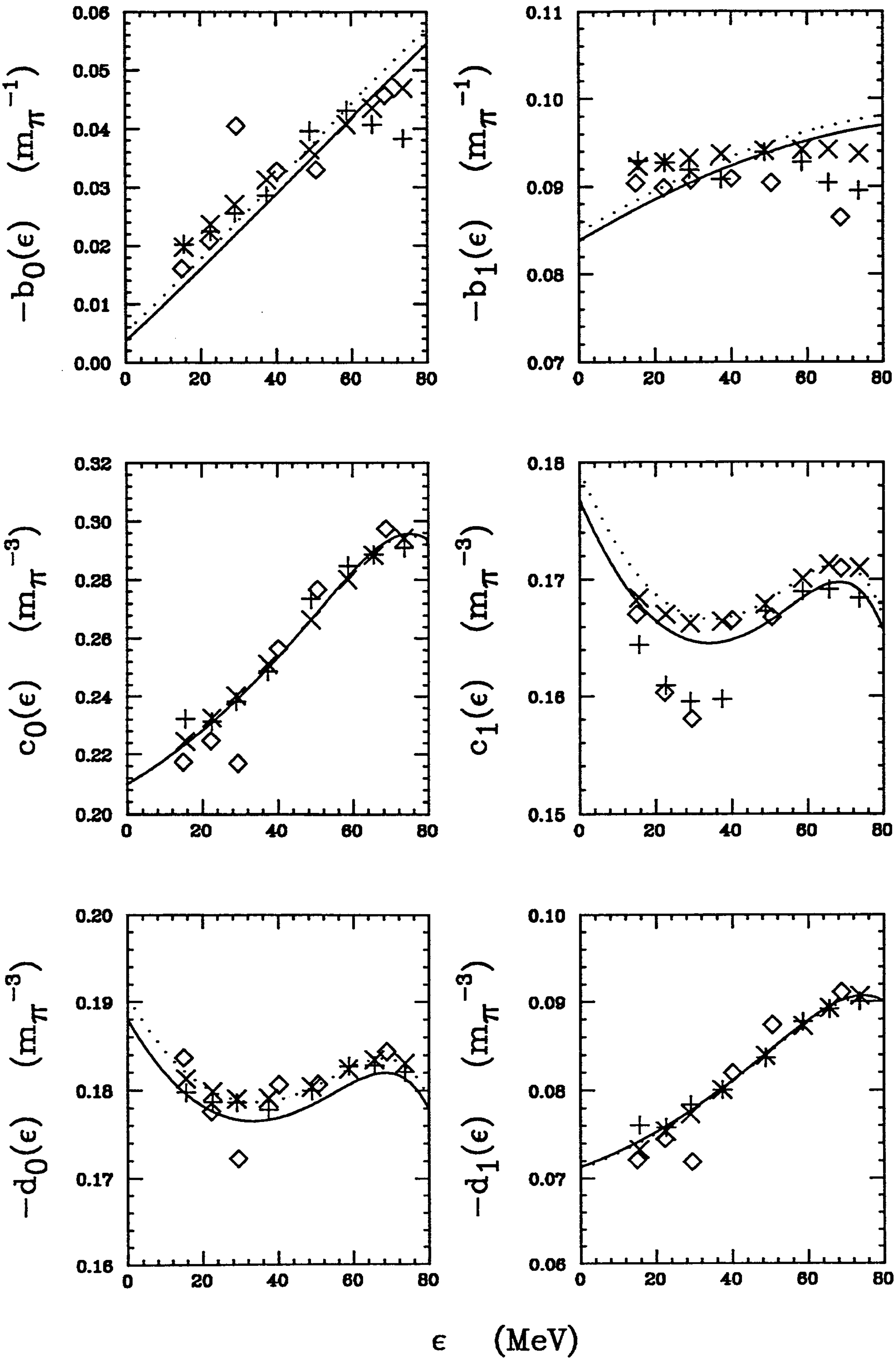

$-b_0(\epsilon)$ (m_π^{-1})
$-b_1(\epsilon)$ (m_π^{-1})
$c_0(\epsilon)$ (m_π^{-3})
$c_1(\epsilon)$ (m_π^{-3})
$-d_0(\epsilon)$ (m_π^{-3})
$-d_1(\epsilon)$ (m_π^{-3})
0 20 40 60 80
ϵ (MeV)

Fig. 3(a)

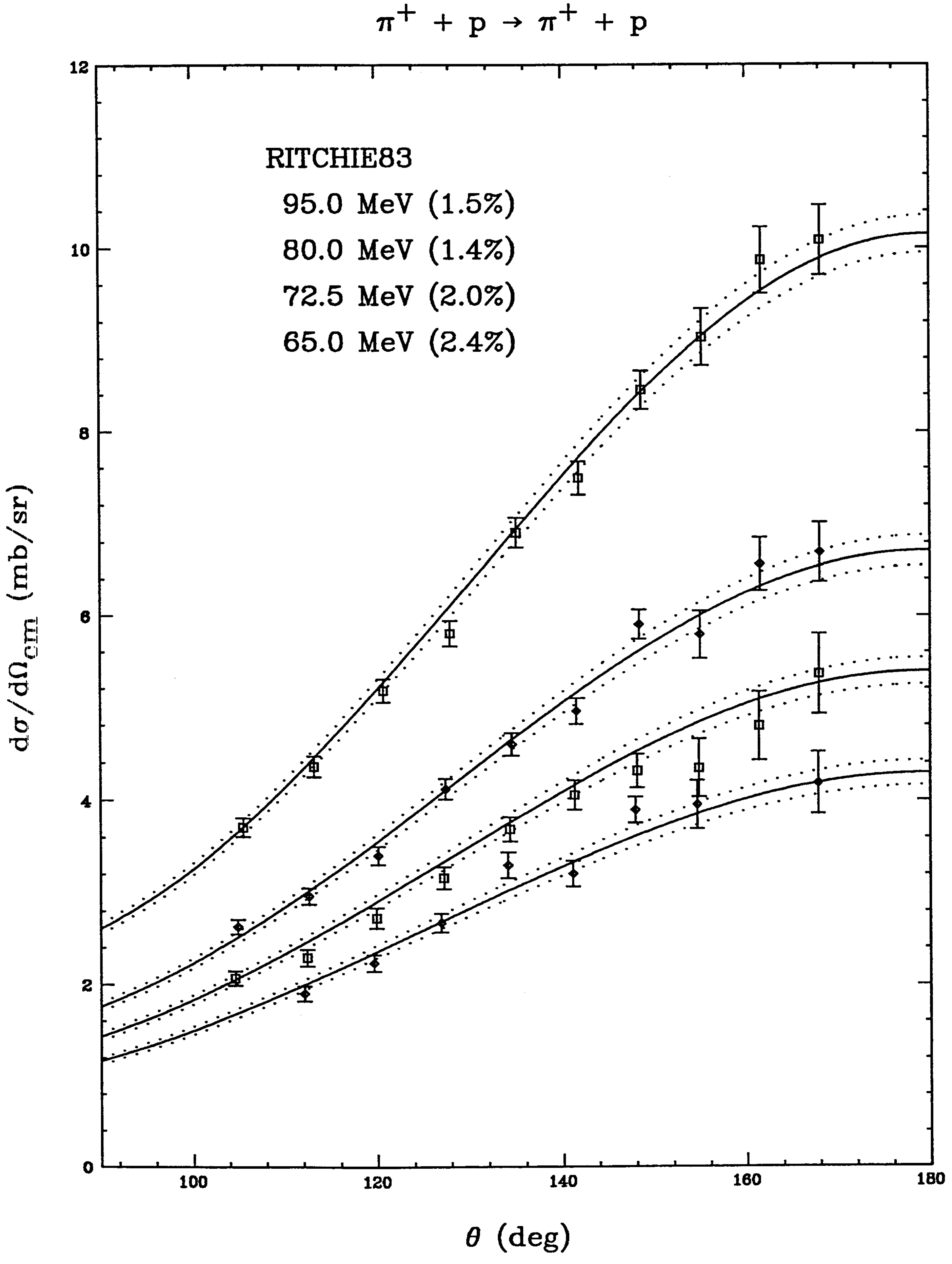

π⁺ + p → π⁺ + p
RITCHIE83
95.0 MeV (1.5%)
80.0 MeV (1.4%)
72.5 MeV (2.0%)
65.0 MeV (2.4%)
dσ/dΩ_cm (mb/sr)
θ (deg)
0
2
4
6
8
10
12
100
120
140
160
180

Fig. 3(b)

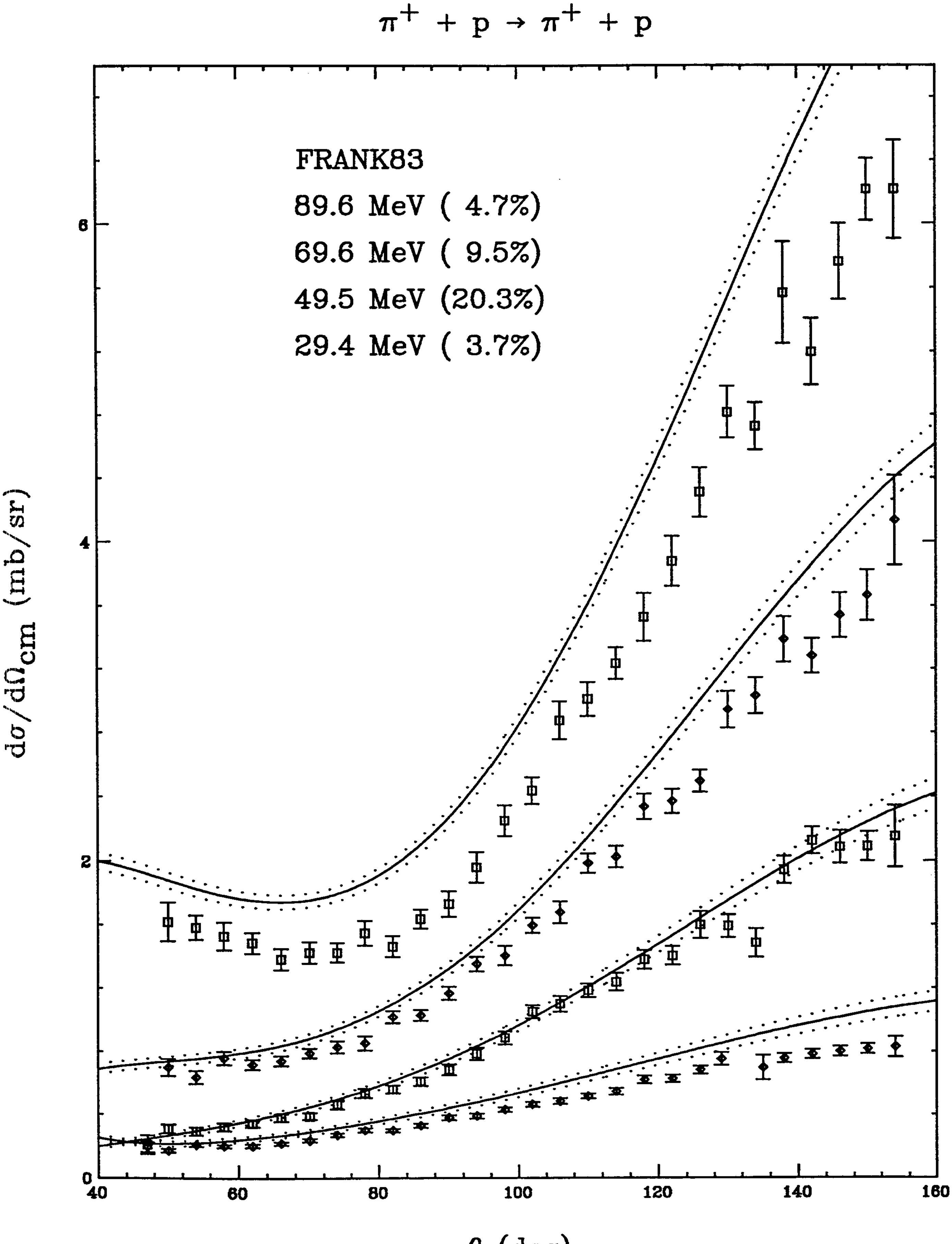

π⁺ + p → π⁺ + p
FRANK83
89.6 MeV (4.7%)
69.6 MeV (9.5%)
49.5 MeV (20.3%)
29.4 MeV (3.7%)
dσ/dΩcm (mb/sr)
θ (deg)
0
2
4
6
40
60
80
100
120
140
160

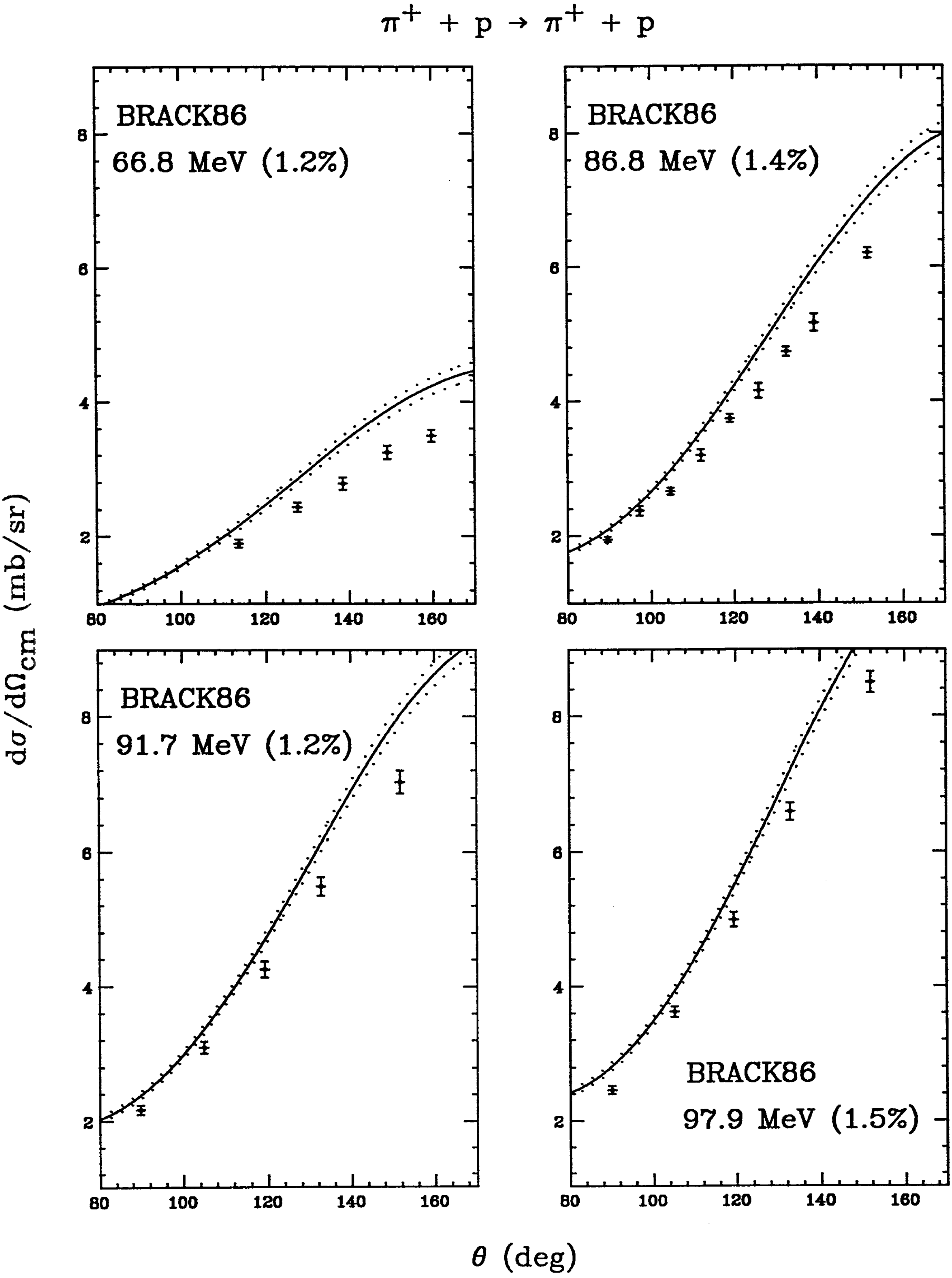
$\pi^+ + p \to \pi^+ + p$
BRACK86
66.8 MeV (1.2%)
BRACK86
86.8 MeV (1.4%)
BRACK86
91.7 MeV (1.2%)
BRACK86
97.9 MeV (1.5%)
$d\sigma/d\Omega_{cm}$ (mb/sr)
θ (deg)
80
100
120
140
160
2
4
6
8

Fig. 3(d)

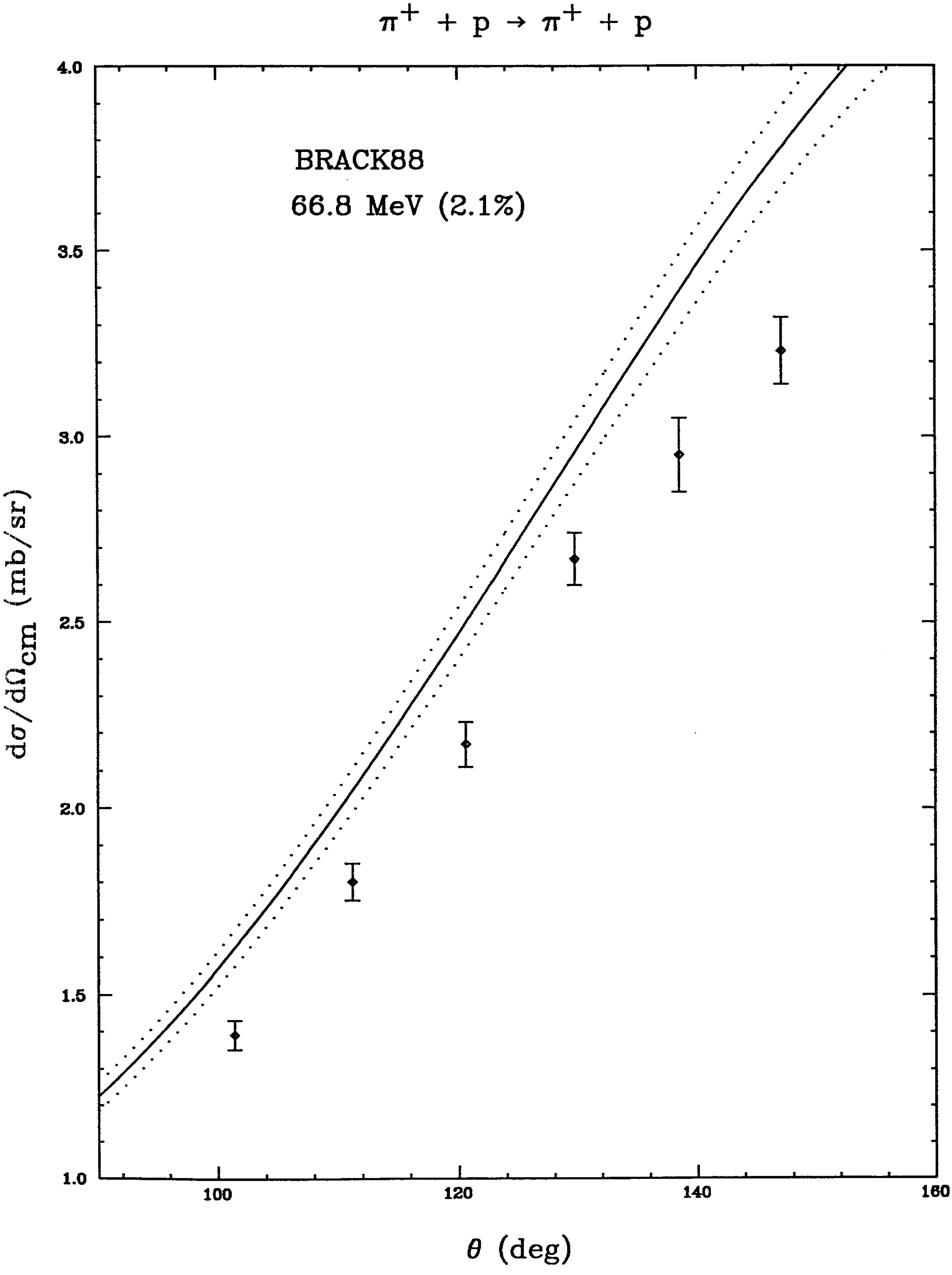

π⁺ + p → π⁺ + p
BRACK88
66.8 MeV (2.1%)
4.0
3.5
3.0
2.5
2.0
1.5
1.0
dσ/dΩcm (mb/sr)
100
120
140
160
θ (deg)

Fig. 3(e)

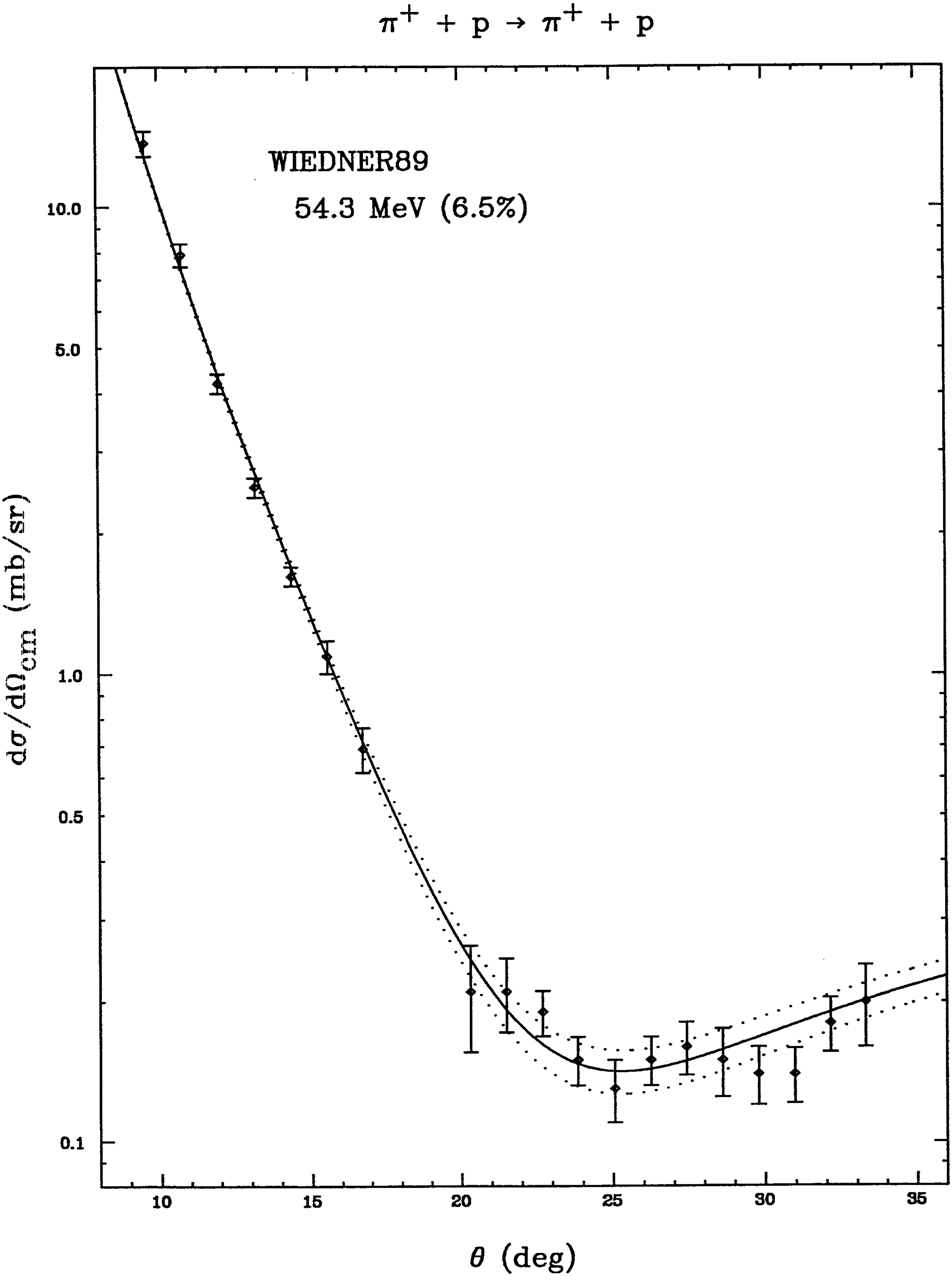
$\pi^+ + p \rightarrow \pi^+ + p$
WIEDNER89
54.3 MeV (6.5%)
$d\sigma/d\Omega_{cm}$ (mb/sr)
10.0
5.0
1.0
0.5
0.1
10
15
20
25
30
35
θ (deg)

Fig. 3(f)

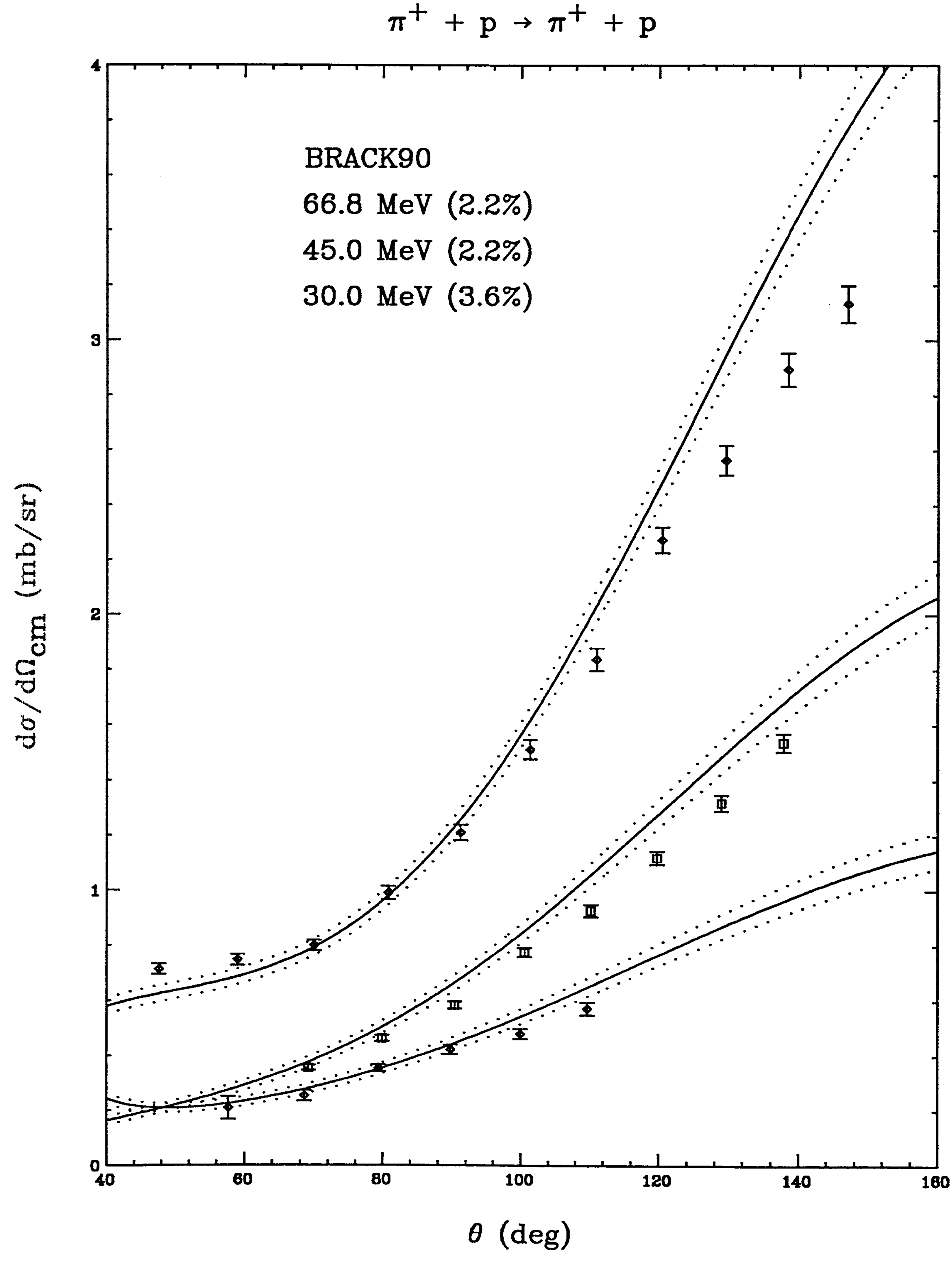

$\pi^+ + p \rightarrow \pi^+ + p$
BRACK90
66.8 MeV (2.2%)
45.0 MeV (2.2%)
30.0 MeV (3.6%)
$d\sigma/d\Omega_{cm}$ (mb/sr)
θ (deg)
0
1
2
3
4
40
60
80
100
120
140
160

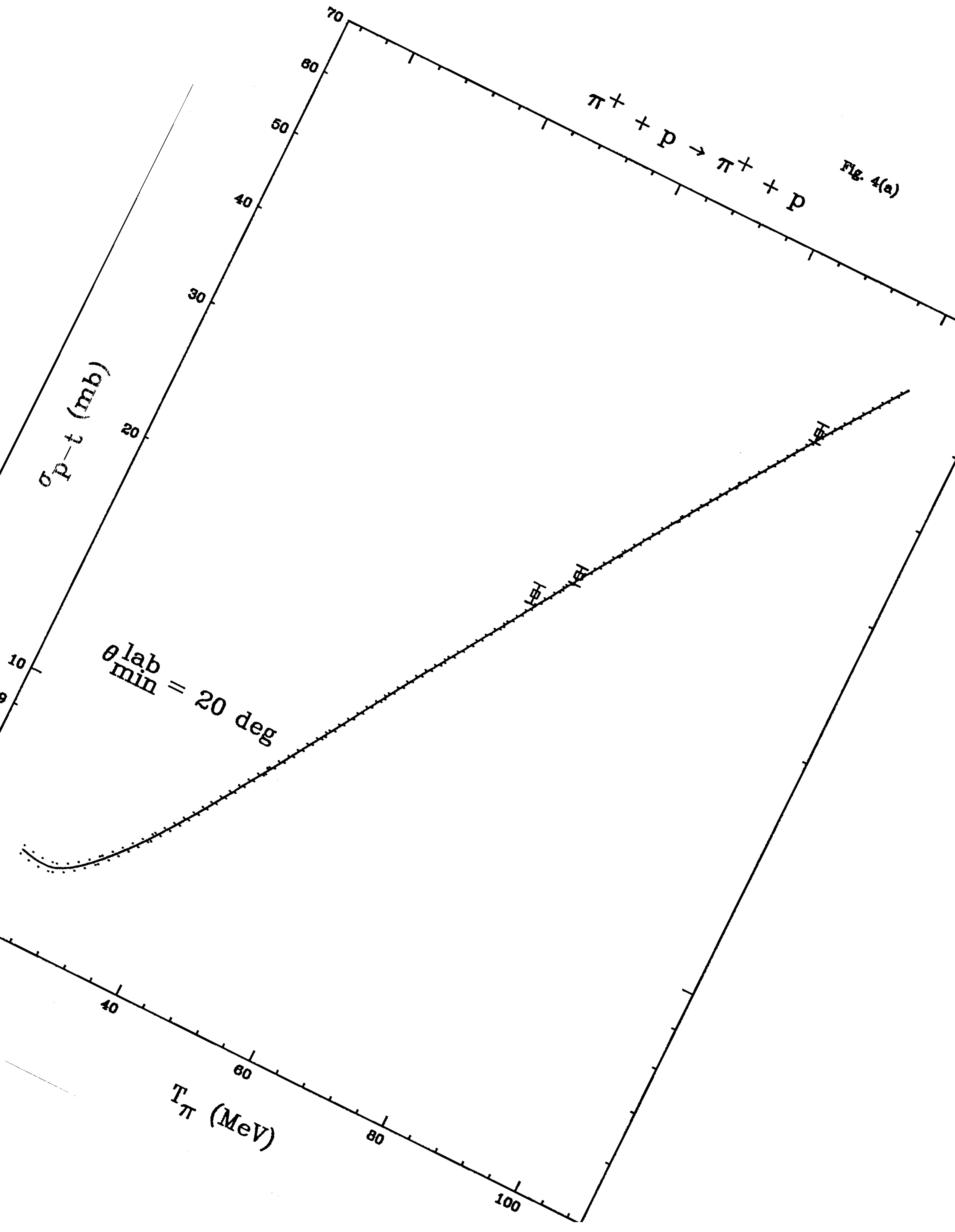

π+ + p → π+ + p
σp–t (mb)
θ lab min = 20 deg
T π (MeV)
70
60
50
40
30
20
10
9
40
60
80
100

Fig. 4(a)

Fig. 4(b)

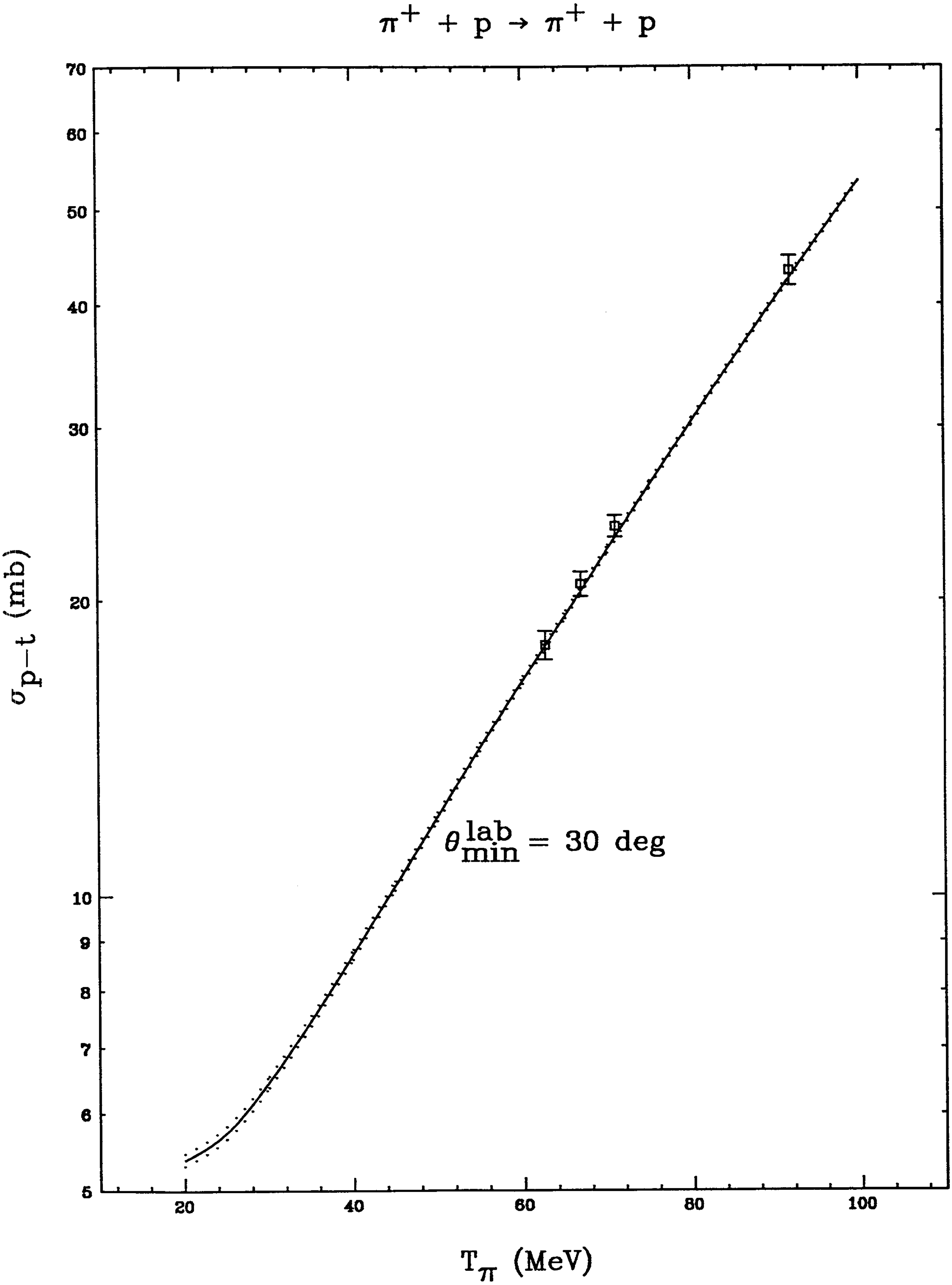
$\pi^+ + p \rightarrow \pi^+ + p$
$\theta_{min}^{lab} = 30$ deg
σ_{p-t} (mb)
T_π (MeV)
70
60
50
40
30
20
10
9
8
7
6
5
20
40
60
80
100

Fig. 5

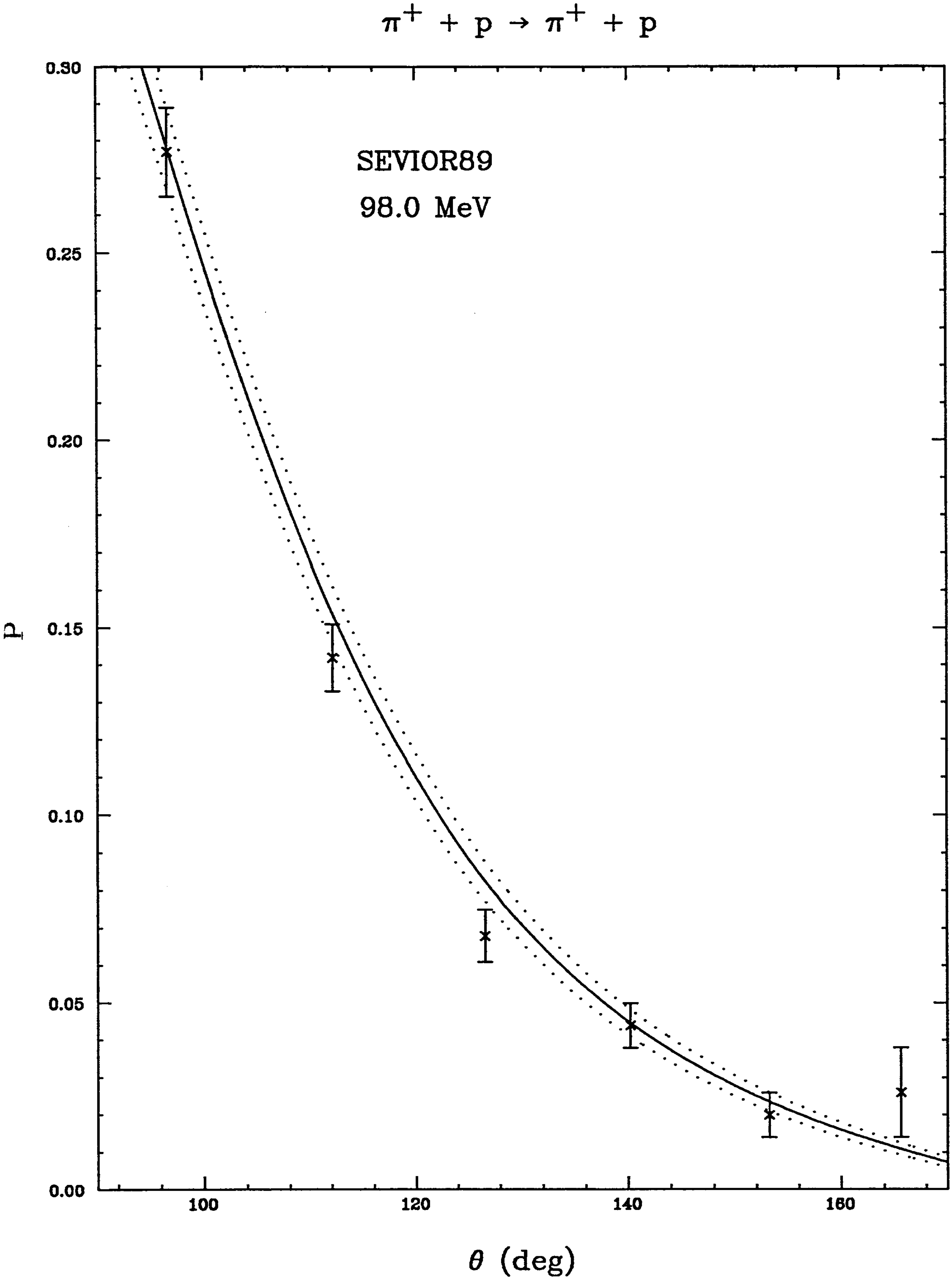

$\pi^+ + p \rightarrow \pi^+ + p$
SEVIOR89
98.0 MeV
0.30
0.25
0.20
0.15
0.10
0.05
0.00
P
100
120
140
160
θ (deg)

$\pi^- + p \rightarrow \pi^- + p$

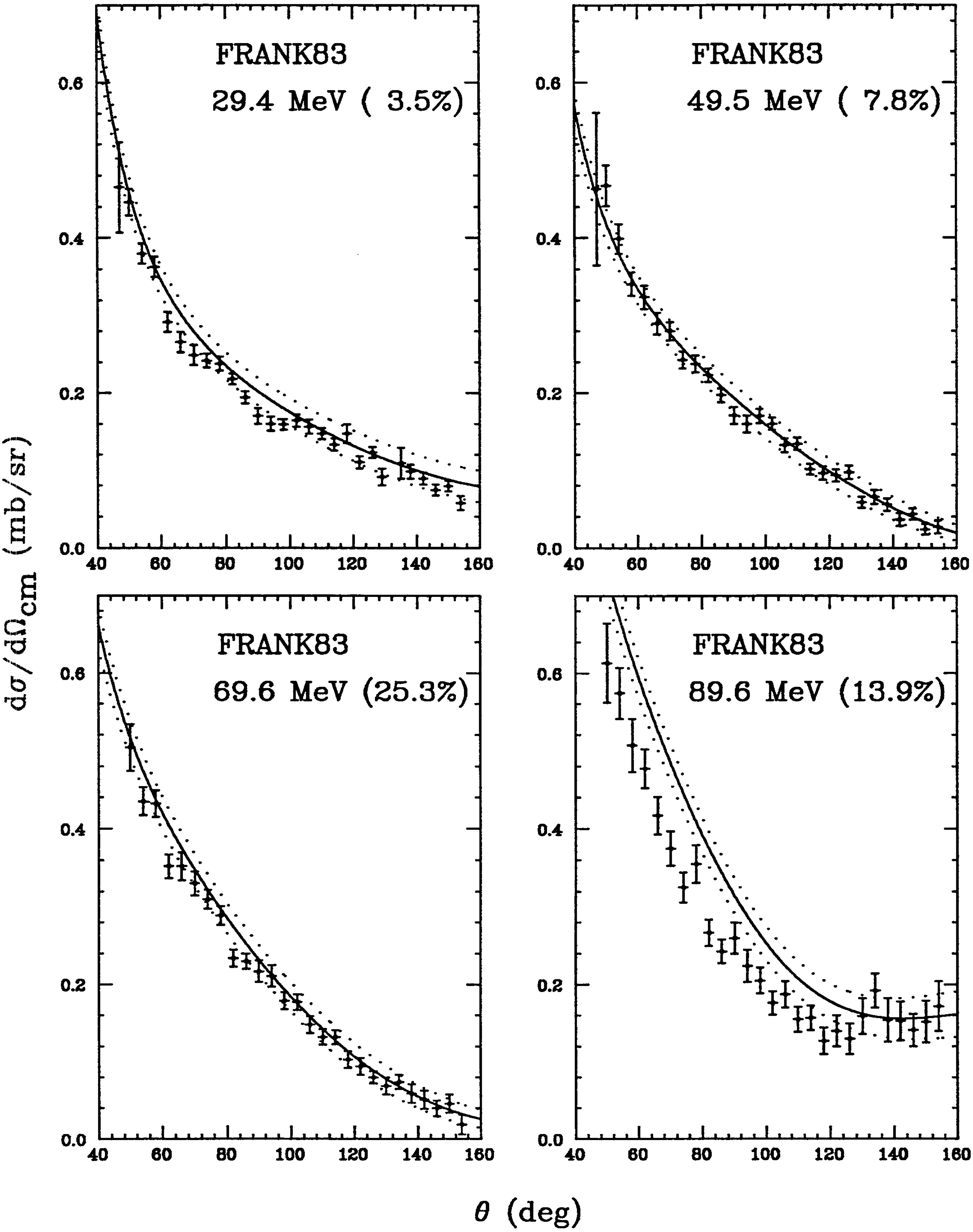

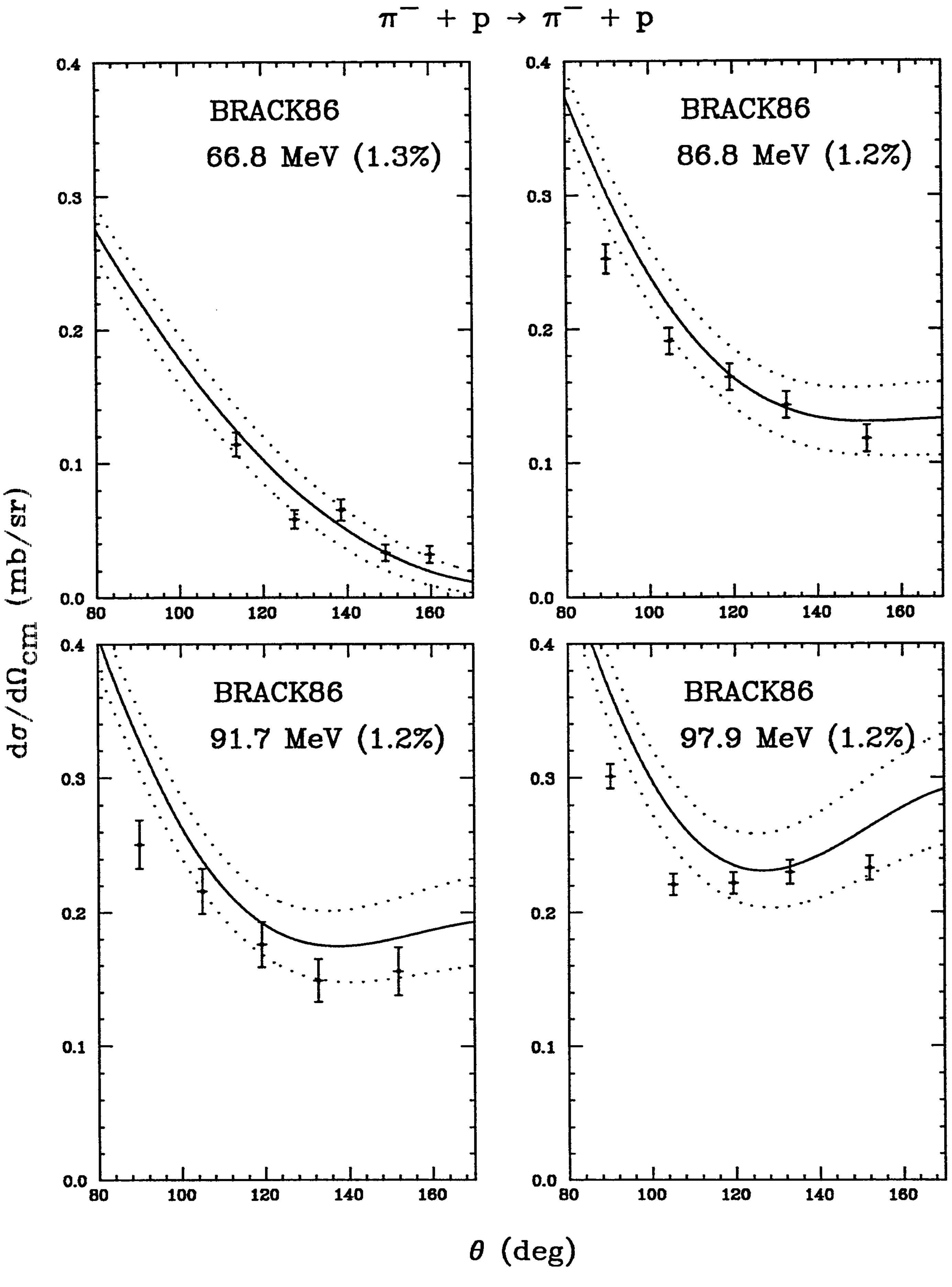
$\pi^- + p \to \pi^- + p$
BRACK86
66.8 MeV (1.3%)
BRACK86
86.8 MeV (1.2%)
BRACK86
91.7 MeV (1.2%)
BRACK86
97.9 MeV (1.2%)
$d\sigma/d\Omega_{cm}$ (mb/sr)
θ (deg)
0.0
0.1
0.2
0.3
0.4
80
100
120
140
160

Fig. 6(c)

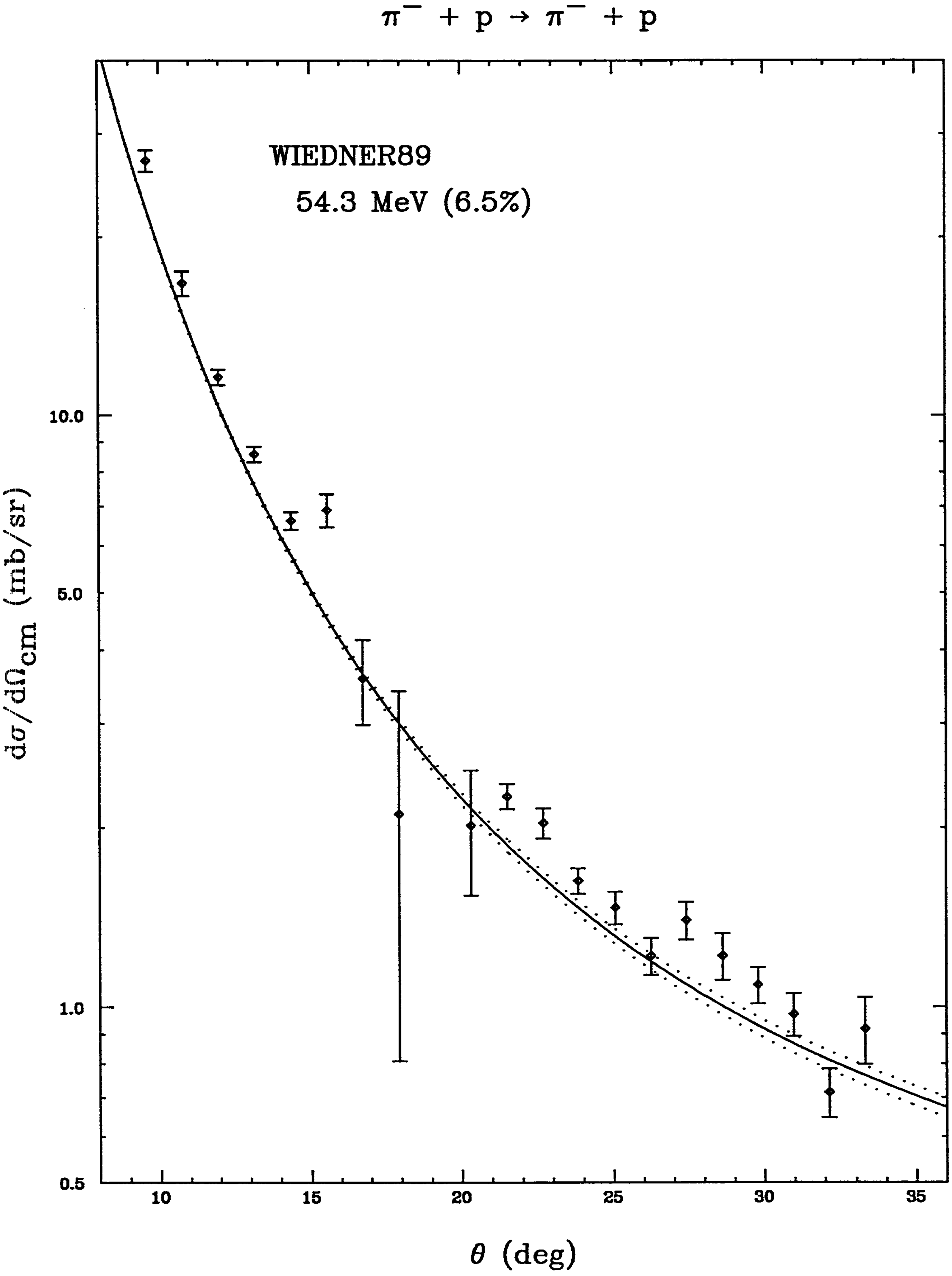

π⁻ + p → π⁻ + p
WIEDNER89
54.3 MeV (6.5%)
10.0
5.0
1.0
0.5
10
15
20
25
30
35
dσ/dΩcm (mb/sr)
θ (deg)

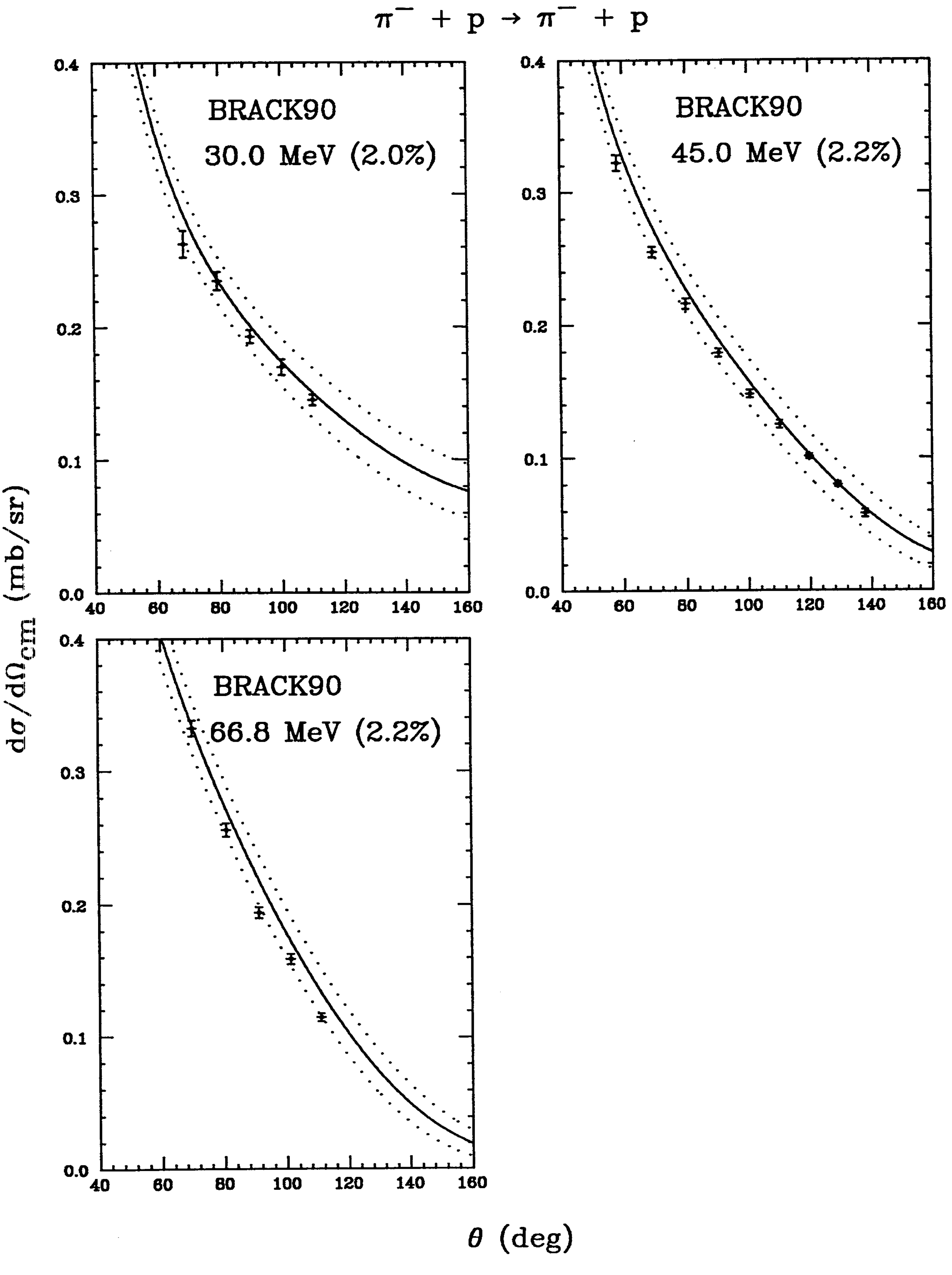
π⁻ + p → π⁻ + p
BRACK90
30.0 MeV (2.0%)
BRACK90
45.0 MeV (2.2%)
BRACK90
66.8 MeV (2.2%)
dσ/dΩcm (mb/sr)
θ (deg)
0.0
0.1
0.2
0.3
0.4
40
60
80
100
120
140
160

Fig. 7

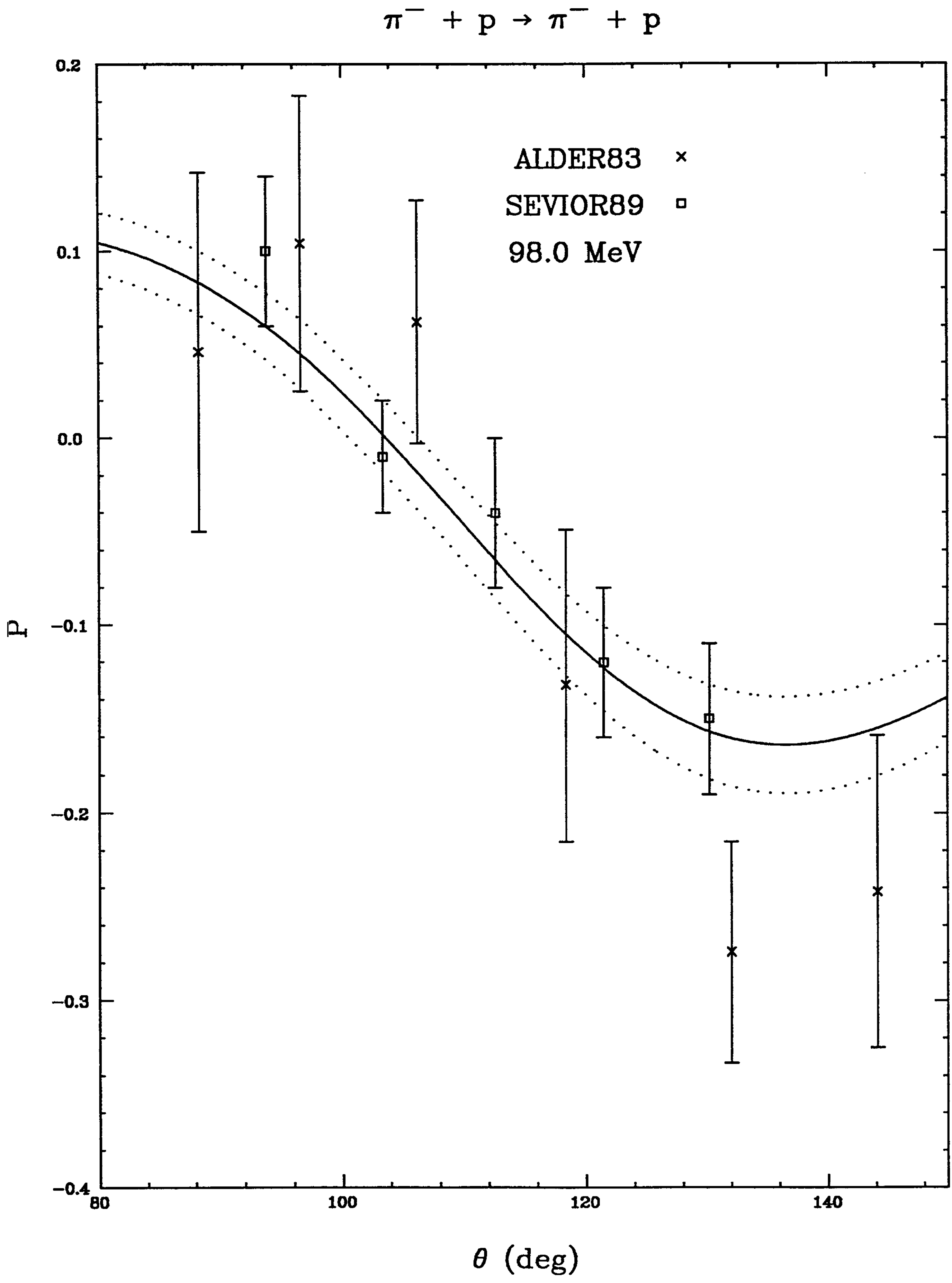

π⁻ + p → π⁻ + p
ALDER83 ×
SEVIOR89 □
98.0 MeV
0.2
0.1
0.0
−0.1
−0.2
−0.3
−0.4
P
80
100
120
140
θ (deg)

Figs. 8

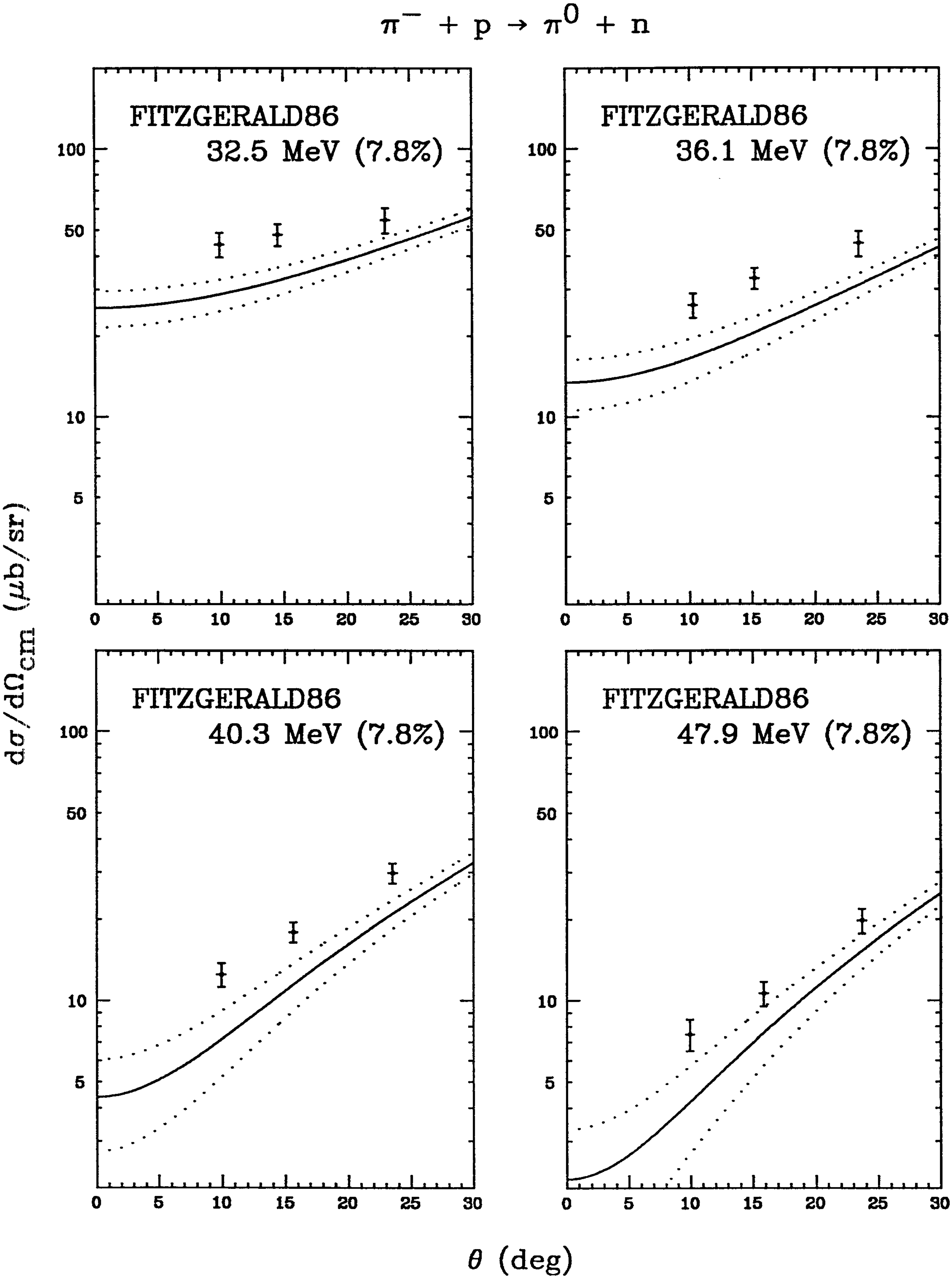

π⁻ + p → π⁰ + n
FITZGERALD86
32.5 MeV (7.8%)
FITZGERALD86
36.1 MeV (7.8%)
FITZGERALD86
40.3 MeV (7.8%)
FITZGERALD86
47.9 MeV (7.8%)
dσ/dΩcm (μb/sr)
θ (deg)

Figs. 8

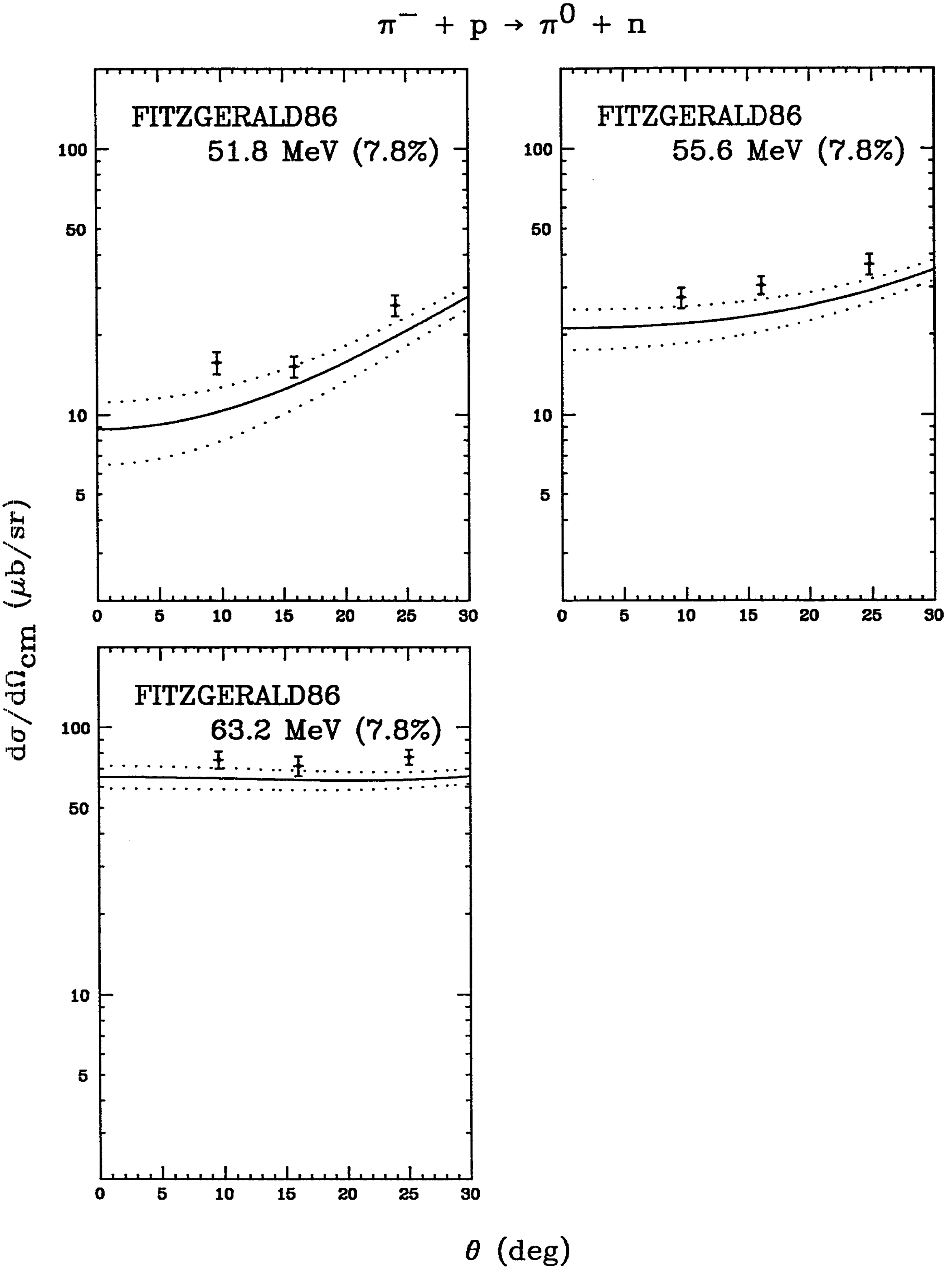

$\pi^- + p \rightarrow \pi^0 + n$
FITZGERALD86
51.8 MeV (7.8%)
FITZGERALD86
55.6 MeV (7.8%)
FITZGERALD86
63.2 MeV (7.8%)
100
50
10
5
0
5
10
15
20
25
30
$d\sigma/d\Omega_{cm}$ (μb/sr)
θ (deg)

Fig. 9

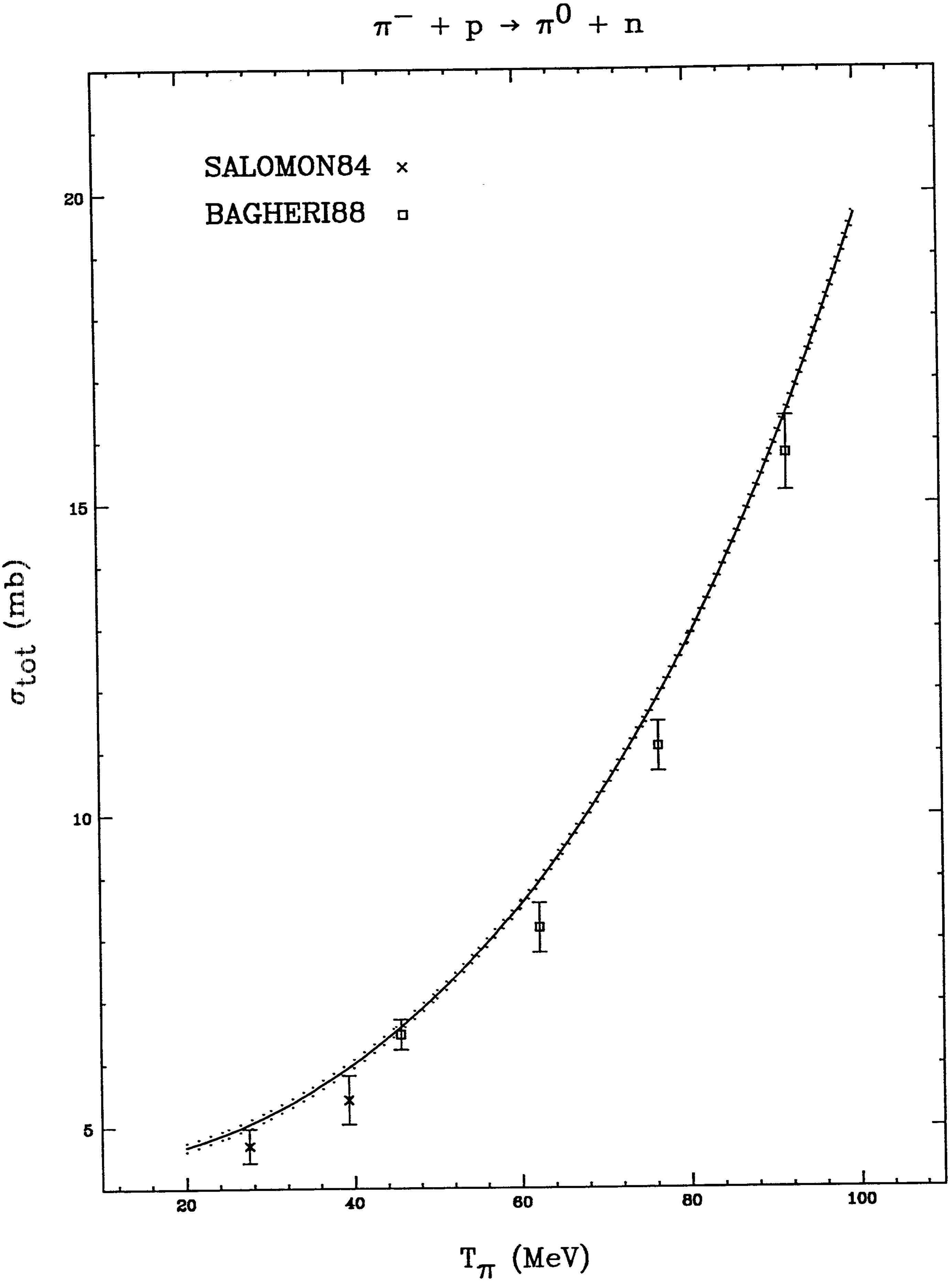

$\pi^- + p \to \pi^0 + n$
SALOMON84 ×
BAGHERI88 □
20
15
10
5
20
40
60
80
100
σ_{tot} (mb)
T_π (MeV)

Captions on the tables

Table 1:

The parameters of our model for two phase-shift solutions. $G_\rho^{(V)}$ is fixed at Pietarinen's value. The errors, shown, are statistical only. The columns correspond to the cases:

a) fit to the KH80 solution [6] and

b) fit to the KA85 solution [8].

G_σ is given in GeV^{-2}.

Table 2:

Measurements of the differential cross section for the elastic $\pi^+ p$ and $\pi^- p$ and for the single-charge-exchange (SCX) reactions. T_π (in MeV) denotes the pion lab kinetic energy and θ (in degrees) stands for the CM scattering angle. The normalization uncertainties N (in %) are also quoted.

Table 3:

Measurements of the asymmetry parameter $A(\theta)$ for the elastic $\pi^+ p$ and $\pi^- p$ reactions. T_π (in MeV) denotes the pion lab kinetic energy and θ (in degrees) stands for the CM scattering angle.

	Fit to the KH80 solution	Fit to the KA85 solution
G_σ	24.3 ± 2.0	24.4 ± 1.4
κ	2.30 ± 0.12	2.23 ± 0.14
$g_{\pi NN}$	12.965 ± 0.076	13.075 ± 0.054
x	0.0361 ± 0.0052	0.0390 ± 0.0028
$g_{\pi N\Delta}$	30.26 ± 0.19	30.28 ± 0.10
Z	-0.329 ± 0.088	-0.361 ± 0.062
χ^2/NDF	0.84	0.33

Table 1

Reaction	Experiment	T_π	θ	N	Reference
π^+p	RITCHIE83 (LAMPF)	65.0 - 95.0	104.6 - 168.1	1.4 - 2.4	[13]
elastic	FRANK83 (LAMPF)	29.4 - 89.6	47.0 - 154.0	3.7 - 20.3	[14]
	BRACK86 (TRIUMF)	66.8 - 97.9	89.6 - 159.7	1.2 - 1.5	[15]
	BRACK88 (TRIUMF)	66.8	101.4 - 147.1	2.1	[16]
	WIEDNER89 (PSI)	54.3	9.6 - 33.3	6.5	[17]
	BRACK90 (TRIUMF)	30.0 - 66.8	47.6 - 147.0	2.2 - 3.6	[18]
π^-p	FRANK83 (LAMPF)	29.4 - 89.6	47.0 - 154.0	3.5 - 25.3	[14]
elastic	BRACK86 (TRIUMF)	66.8 - 97.9	89.6 - 159.7	1.2 - 1.3	[15]
	WIEDNER89 (PSI)	54.3	9.6 - 33.3	6.5	[17]
	BRACK90 (TRIUMF)	30.0 - 66.8	58.2 - 137.8	2.0 - 2.2	[18]
SCX	FITZGERALD86 (LAMPF)	32.5 - 63.2	9.6 - 25.0	7.8	[23]

Table 2

Reaction	Experiment	T_π	θ	Reference
π^+p elastic	SEVIOR89 (TRIUMF)	98.0	96.7 - 165.6	[21]
π^-p	ALDER83 (PSI)	98.0	88.3 - 144.1	[22]
elastic	SEVIOR89 (TRIUMF)	98.0	93.8 - 130.2	[21]

Table 3